Magnetic order and $5d^1$ multipoles in a rhenate double perovskite Ba_2MgReO_6

S. W. Lovesey[1,2] and D. D. Khalyavin[1]
[1]*ISIS Facility, STFC, Didcot, Oxfordshire OX11 0QX, United Kingdom*
[2]*Diamond Light Source Ltd, Didcot, Oxfordshire OX11 0DE, United Kingdom*

(Received 29 April 2021; revised 5 June 2021; accepted 7 June 2021; published 25 June 2021)

Structural and magnetic transitions in a double perovskite hosting $5d^1$ Re ions are discussed in the context of recently published high-resolution x-ray diffraction patterns [D. Hirai *et al.*, Phys. Rev. Res. **2**, 022063(R) (2020)]. Our symmetry-inspired analysis of a reported structural transition below room temperature, from cubic to tetragonal symmetry, reveals order of a lone E_g-type charge quadrupole. A magnetic motif at lower temperature is shown to be composed of two order parameters, with propagation vectors $\mathbf{k} = (0, 0, 1)$ and $\mathbf{k} = (0, 0, 0)$, which imply a magnetic space group $Pnn'm'$. A concomitant lowering of Re site symmetry adds a T_{2g} type to permitted quadrupoles. Findings from our studies, for structural and magnetic properties of Ba_2MgReO_6, surface in predicted amplitudes for x-ray diffraction at rhenium L_2 and L_3 absorption edges, and magnetic neutron Bragg diffraction. Specifically, entanglement of anapole and spatial degrees of freedom creates a quadrupole in the neutron scattering amplitude. It would be excluded in an unexpected scenario whereby the rhenium atomic state is adequately described by a single value of the total angular momentum. Quadrupoles in x-ray and neutron diffraction amplitudes possess different angular symmetries, since the former is purely electronic and the latter purely magnetic. A chiral signature visible in resonant x-ray diffraction will be one consequence of predicted chargelike quadrupole and magnetic dipole orders. A model Re wave function consistent with all current knowledge is a guide to electronic and magnetic multipoles engaged in x-ray and neutron diffraction investigations.

DOI: 10.1103/PhysRevB.103.235160

I. INTRODUCTION

Electronic and magnetic properties of double perovskites hosting heavy transitions metal ions are popular topics of research. Compounds in the news include Ba_2MgReO_6 [1,2], Ba_2BOsO_6 with B = Zn, Mg, Ca [3,4], Ba_2YReO_6 [5,6], and Sr_2MgReO_6 [7]. The spin-orbit coupling in the single-ion Hamiltonian increases in magnitude as Z^4 to a good approximation, where Z is the atomic number. For $5d$ systems it is of a similar order of magnitude to both the Hund's and crystal field terms, and a range of behaviors can be realized depending on the balance between these and the magnetic exchange (the coupling constant).

The heavy transition ions possess electronic and magnetic multipoles that deflect beams of neutrons and x rays. In addition to conventional magnetic dipoles, formed by expectation values of spin **S** and orbital **L** operators, there is evidence of quadrupoles and octupoles [1–6]. If ions occupy acentric sites, Dirac multipoles are permitted in both neutron and x-ray diffraction, e.g., a spin anapole $\mathbf{\Omega} = (\mathbf{S} \times \mathbf{R})$ where **R** is the position operator [8–10]. A quadrupole formed from **R** and **Ω** is capable of deflecting neutrons [11].

The present study of Ba_2MgReO_6 includes proposals for additional x-ray diffraction experiments whose significance might have been overlooked, and calculations of magnetic neutron scattering amplitudes, again for future experiments. A structural phase transition from cubic to tetragonal as the sample temperature passes through ≈33 K, and long-range magnetic order below ≈18 K, are conclusions based on studies of single crystals using conventional (Thomson) and resonant x-ray diffraction by Hirai *et al.* [2]. Notably, the authors do not include expressions for relevant scattering amplitudes in their publication. In consequence, associations between measured intensities of Bragg spots and Re magnetic dipoles and chargelike quadrupoles—the principal topic of the publication [2]—are made by inference and simple arguments. We make good the noted shortcomings with a comprehensive calculation of all relevant scattering amplitudes for Ba_2MgReO_6 using spatial and magnetic symmetry, and atomic physics. Rhenium ions occupy centrosymmetric sites in tetragonal $P4_2/mnm$ that supports a lone quadrupole type, and the experimental evidence is that magnetic dipoles lie in the basal plane [1,2]. Regarding the existence and classification of chargelike quadrupoles, we conclude that one symmetry type is allowed in the tetragonal structure ($P4_2/mnm$) and two types are allowed in the magnetic structure ($Pnn'm'$). Only one symmetry type contributes to basis-forbidden Bragg spots observed in resonant x-ray diffraction, however.

In the next section we elucidate the nature of both the structural and magnetic phase transitions. Thereafter, we classify electronic and magnetic multipoles. The tetragonal paramagnetic structure admits two of five possible chargelike quadrupoles, and the family has an additional member in lower magnetic symmetry. Our findings about quadrupole orders differ from speculations that have been reported [2].

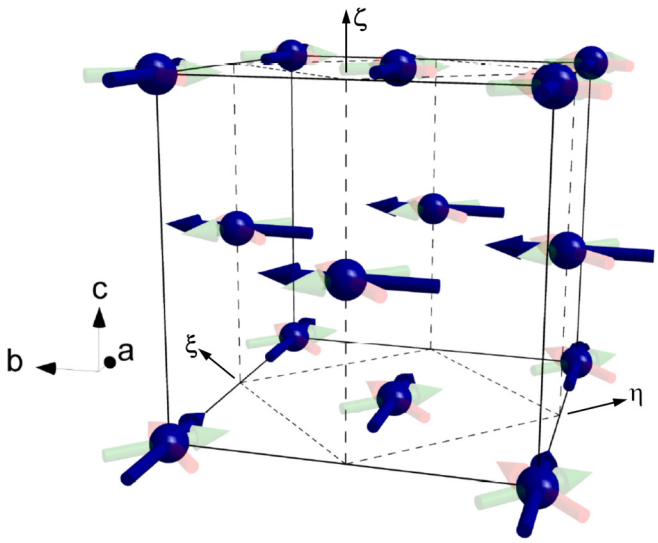

FIG. 1. Ferro- and antiferromagnetic dipole components of the ordered magnetic structure Ba_2MgReO_6 (as determined experimentally in Ref. [2]) are depicted by transparent red and green arrows, respectively. A tetragonal basis labeled (ξ, η, ζ) is introduced in Sec. II.

They can be tested to some extent in azimuthal-angle scans (rotation of the crystal about the reflection vector) using resonance-enhanced x-ray Bragg diffraction. A chiral signature exists as a consequence of the specific magnetic long-range order. Likely, a magnetic quadrupole formed from **R** and **Ω** is permitted, and we calculate the intensity of magnetic neutron scattering to be tested in a future experiment. All mentioned multipoles are evaluated using a simple, but wholly feasible, Re atomic wave function. Alternative estimates can be obtained from a tried and tested package for the simulation of electronic structure [12].

II. MATERIAL PROPERTIES

The paramagnetic phase of Ba_2MgReO_6 is described by a tetragonal space-group $P4_2/mnm$ (No. 136, crystal class $4/mmm$) with Re ions at sites $2a$ ($m.mm$ site symmetry) [2]. Cell parameters $a = b \approx 5.7136$ Å and $c \approx 8.0849$ Å. Lattice vectors and origin of the subgroup with respect to the parent cubic structure $Fm\bar{3}\ m$ (No. 225) are $(\frac{1}{2}, -\frac{1}{2}, 0)$, $(\frac{1}{2}, \frac{1}{2}, 0)$, $(0, 0, 1)$, and $(0, 0, 0)$, respectively. Miller indices for the subgroup h, k, l are integers. The propagation vector for the symmetry lowering from cubic to tetragonal is $\mathbf{k} = (0, 0, 1)$, so even if we use the parent cubic cell for indexation, then some of the indices will violate the F-centring condition, but they still will be integers.

Magnetic long-range order is a combination of two order parameters, an antiferro (AFM) associated with $\mathbf{k} = (0, 0, 1)$ and a ferro (FM) associated with $\mathbf{k} = (0, 0, 0)$. The two orders are depicted in Fig. 1, and their individual symmetries are [13]

(AFM) P_Innm (BNS setting, No. 58.404), basis $= \{(0, 0, 1), (\frac{1}{2}, \frac{1}{2}, 0), (-\frac{1}{2}, \frac{1}{2}, 0)\}$, origin at (0, 0, 0), Re use sites $2a$,

(FM) $Im'm'm$ (No. 71.536), basis $= \{(0, 0, -1), (-\frac{1}{2}, \frac{1}{2}, 0), (\frac{1}{2}, \frac{1}{2}, 0)\}$, origin at (0, 0, 0), Re use sites $2a$.

The presence of both order parameters implies that the symmetry of the magnetic phase is $Pnn'm'$ (No. 58.398, magnetic crystal-class $mm'm'$), using a basis $\boldsymbol{\xi} = (\frac{1}{2}, \frac{1}{2}, 0)$, $\boldsymbol{\eta} = (-\frac{1}{2}, \frac{1}{2}, 0)$, $\boldsymbol{\zeta} = (0, 0, 1)$, origin (0, 0, 0), and Re in sites $2a$ with symmetry $2'/m'$. A spontaneous magnetization is permitted in the magnetic crystal class. Also, a nonlinear magnetoelectric effect is due to an invariant of the type HEE alone. Such symmetry is permitted for rare-earth garnets and a nonlinear effect has been observed.

An interesting point is that the magnetic space group allows the structural distortions with the $P4_2/mnm$ symmetry. This means that there must be a coupling between the AFM, FM, and these structural distortions. Specifically, there is a trilinear free-energy invariant which is just a product of three order parameters $\propto \{\sigma \bullet \lambda \bullet \mu\}$, with σ-structural distortions, λ-AFM and μ-FM order parameters. This energy term indicates that in the presence of the $P4_2/mnm$ structural distortions, a condensation of AFM order will induce FM component and vice versa (FM will necessarily induce AFM). This makes the scenario to be symmetry consistent.

Regarding symmetry of the quadrupoles in the tetragonal phase, we calculated the subduction frequency (multiplicity) for the $2a$ site symmetry irreducible representations (irreps) in the space group representation $X2+$ which reduces symmetry down to $P4_2/mnm$. Such a calculation indicates local distortions (associated with which site symmetry irreps) in the global tetragonal distortions. The two-dimensional E_g site irrep has a nonzero subduction frequency, while the subduction frequency of the three-dimensional T_{2g} site irrep is zero. Specifically, T_{2g}-type quadrupoles, defined in the cubic (a, b, c) basis ($Fm\bar{3}\ m$) depicted in Fig. 1, cannot drive the transition to $P4_2/mnm$. In fact, T_{2g} distortions are secondary and associated with $\mathbf{k} = (0, 0, 0)$, meaning some ferro ordering of the T_{2g}-type quadrupoles should be allowed but they cannot drive the structural transition.

III. MULTIPOLES

Rhenium ions occupy sites with inversion symmetry and all multipoles $\langle t^K{}_Q\rangle$, with rank K and projections $-K \leqslant Q \leqslant K$ are axial (parity even). The complex conjugate of our multipoles satisfy $\langle t^K{}_{-Q}\rangle = (-1)^Q \langle t^K{}_Q\rangle^*$ and the diagonal $\langle t^K{}_0\rangle$ is purely real, with a phase convention $\langle t^K{}_Q\rangle = [\langle t^K{}_Q\rangle' + i\langle t^K{}_Q\rangle'']$ for real and imaginary parts labeled by single and double primes, respectively. Cartesian and spherical components of a dipole $\mathbf{R} = (x, y, z)$ are related by $x = (R_{-1} - R_{+1})/\sqrt{2}, y = i(R_{-1} + R_{+1})/\sqrt{2}, z = R_0$. For the paramagnetic state, contiguous to long-range magnetic order in the phase diagram, we use $P4_2/mnm$ (No. 136), for which $Q = 2n$ and $(-1)^n \langle t^K{}_{-Q}\rangle = \langle t^K{}_Q\rangle$ with n a whole integer. Rank K is even for chargelike multipoles viewed in x-ray diffraction enhanced by electric dipole–electric dipole ($E1{-}E1; 2p \leftrightarrow 5d$) or electric quadrupole–electric quadrupole ($E2{-}E2; 1s, 2s \leftrightarrow 5d$) absorption events, for which the time signature $= (-1)^K$. Applied to quadrupoles, $K = 2$, allowed projections $Q = 0$ and ± 2. Site symmetry permits the diagonal quadrupole $\langle t^2{}_0\rangle$ and one off-diagonal component that is purely imaginary, $\langle t^2{}_{+2}\rangle = -\langle t^2{}_{+2}\rangle^*$, i.e., the quadrupole has $\xi\eta$-like angular symmetry (Γ_5, t_{2g}). In

the magnetic phase, sites $2a$ in $Pnn'm'$ demand $Q + K = 2n$. Thus, allowed $Q = 0$ and ± 2 for $K = 2$, with no additional constraint from site symmetry on the off-diagonal $\langle t^2{}_{\pm 2}\rangle$. Using cubic axes (a, b, c) for the moment, an E_g (Γ_3) quadrupole with $(x^2 - y^2)$ angular symmetry exists in the paramagnetic phase in the temperature interval ≈18–33 K, and magnetic order allows addition of a T_{2g} (Γ_5) quadrupole with xy angular symmetry.

A plausible rhenium atomic wave function, based on the configuration $5d^1$ (Re^{6+}, $S = \frac{1}{2}$, $L = 2$), has twofold rotation symmetry about the crystal c axis, and yields a magnetic dipole confined to the ξ-η plane, as in Fig. 1. Quadrupoles in the paramagnetic phase impose an additional constraint. Candidate wave functions are linear combinations of d-orbitals d_m, with projections $-2 \leqslant m \leqslant 2$ that we define with respect to a rhombically distorted octahedron with axes parallel to lines joining the central Re ion to each pair of O ligand ions. Suitable combinations of orbitals are d_0 and $d_{\pm 2}$, or d_{+1} and d_{-1}. We elect to use a minimal model, for more than illustrative purposes, defined by $|u\rangle = [\alpha d_0 + \beta d_{+2}]$ with α purely real, $\beta = (\beta' + i\beta'')$ and $\alpha^2 + |\beta|^2 = 1$ for normalization. We shall find that orbital angular momentum is quenched, and α is fixed by the spin moment in the ξ-η plane. Off-diagonal, chargelike quadrupoles arise from an admixture of d orbitals, while $[\alpha^2 - |\beta|^2]$ measures the total strength of the diagonal quadrupole. In the magnetic phase there are two unknowns, α and β', say, while site symmetry in paramagnetic $P4_2/mnm$ requires $\beta'' = 0$.

Saturation values of magnetic multipoles are calculated with a normalized ground state $|g\rangle = [|u\rangle + \exp(i\phi)|\hat{u}\rangle]/\sqrt{2}$, where $|\hat{u}\rangle$ is the conjugate component of the Kramers doublet, and the angle ϕ specifies orientation of dipoles in the ξ-η plane. Composite spin-orbital states required in $|u\rangle$ are best represented by total angular momenta using $j = 3/2$, $j' = 5/2$, and two projections $m = 1/2$, $m' = 5/2$ (S-L coupling scheme),

$$d_0 \uparrow = [\sqrt{2}|jm\rangle + \sqrt{3}|j'm\rangle]/\sqrt{5}, \quad d_{+2} \uparrow = |j'm'\rangle. \tag{1}$$

Multipoles $\langle t^K{}_Q\rangle$ in orthogonal coordinates (ξ, η, ζ) for the tetragonal cell are related to $\langle T^K{}_Q\rangle = \langle g|T^K{}_Q|g\rangle$ by a rotation about the ζ axis through 45 °, namely, $\langle t^K{}_Q\rangle = \exp(iQ\pi/4)\langle T^K{}_Q\rangle$. The construction of $|g\rangle$ ensures $\langle t^1{}_\zeta\rangle = \langle t^1{}_0\rangle = 0$. In the paramagnetic phase, $\langle T^2{}_{+2}\rangle = [\alpha\beta\langle d_{+2}|T^2{}_{+2}|d_0\rangle]$ is purely real for real coefficients, whereupon $\langle t^2{}_{+2}\rangle = -\langle t^2{}_{-2}\rangle$ as required by site symmetry. The diagonal quadrupole $\langle t^2{}_0\rangle = [\alpha^2\langle d_0|T^2{}_0|d_0\rangle + |\beta|^2\langle d_{+2}|T^2{}_0|d_{+2}\rangle]$. Turning to the magnetic phase, $\langle \mathbf{L}\rangle = 0$, and spin components are $\langle S_\xi\rangle = [\alpha^2\cos(\pi + 4\phi)/8]$, $\langle S_\eta\rangle = [\alpha^2\sin(\pi + 4\phi)/8]$, $\langle S_\zeta\rangle = 0$. An observed magnetic moment $\approx 0.3\,\mu_B$ implies $\alpha^2 \approx 0.3$ and $\alpha|\beta| \approx \pm 0.46$ [1].

Multipoles observed in resonance enhanced x-ray diffraction have different values at different absorption edges. Dependence on the total angular momentum of the core states, 1/2 for L_2 and 3/2 for L_3, is carried by reduced matrix elements that obey sum rules [8,14]. For L_2 and L_3 edges $\langle \mathbf{t}^1\rangle_{L3} + \langle \mathbf{t}^1\rangle_{L2} = -\langle \mathbf{L}\rangle_d/(10\sqrt{2})$, and $\langle \mathbf{t}^2\rangle_{L3} + \langle \mathbf{t}^2\rangle_{L2} = \langle\{\mathbf{L} \otimes \mathbf{L}\}^2\rangle_d/30$, with $\{\mathbf{L} \otimes \mathbf{L}\}^2{}_0 = [3(L_\zeta)^2 - L(L+1)]/\sqrt{6}$ for the diagonal element of the standard tensor product. The dipole $\langle T^1{}_{+1}\rangle = [\exp(i\phi)\langle u|T^1{}_{+1}|\hat{u}\rangle/2]$, and the matrix element therein for L_2 is denied contributions from j' by the dipole selection rule. On the other hand, there are contributions to the matrix element from both atomic states, j and j', at L_3. Projections $Q = 1, 3, 5$ are allowed in the matrix element $\langle u|T^K{}_Q|\hat{u}\rangle$, which contribute to magnetic octupoles ($K = 3$) and triakontadipoles ($K = 5$).

In summary, our model Re atomic wave function yields the following guides to multipoles observed in diffraction enhanced by an $E1$-$E1$ event,

$$\begin{aligned} L_2 \text{ edge; } \langle T^1{}_{+1}\rangle &= -\exp(i\phi)(1/45)\alpha^2, \\ \langle T^2{}_0\rangle &= -(15\sqrt{6})^{-1}\alpha^2, \quad \langle T^2{}_{+2}\rangle = 0. \end{aligned} \tag{2}$$

$$\begin{aligned} L_3 \text{ edge; } \langle T^1{}_{+1}\rangle &= \exp(i\phi)(1/45)\alpha^2, \\ \langle T^2{}_0\rangle &= (15\sqrt{6})^{-1}[3 - 5\alpha^2], \\ \langle T^2{}_{+2}\rangle &= (5\sqrt{6})^{-1}\alpha\beta^*. \end{aligned}$$

Dipole results fit with quenched orbital angular momentum and the aforementioned dipole sum rule. A successful analysis similar to the one proposed here for strontium iridate uses a ground state for which $\langle \mathbf{t}^1\rangle_{L2} = 0$ [15]. Evidently, experimental results for diffraction at the L_2 edge of Re in Ba_2MgReO_6 would be a valuable asset in determining the atomic ground state. Corresponding estimates of the dipole and quadrupole in the amplitude for magnetic neutron diffraction are listed in Eq. (13).

IV. RESONANT X-RAY DIFFRACTION

The photon scattering length is developed in the small quantity E/mc^2, where E is the primary energy ($mc^2 \approx 0.511$MeV). At the second level of smallness in this quantity it contains resonant processes that may dominate all other contributions should E match an atomic resonance Δ. Assuming that virtual intermediate states are spherically symmetric, to a good approximation, the scattering length $\approx\{F_{\nu\mu}/(E - \Delta + i\Gamma/2)\}$ in the region of the resonance, where Γ is the total width of the resonance. The numerator $F_{\nu\mu}$ is a dimensionless amplitude, or unit-cell structure factor, for Bragg diffraction in the scattering channel with primary (secondary) polarization μ (ν). Henceforth, we use $(\nu\mu)$ in place of $F_{\nu\mu}$ to abbreviate notation. By convention, σ labels polarization normal to the plane of scattering, and π denotes polarization within the plane. In the nominal setting, axis (x, y, z) in which σ polarization is parallel to the z axis and the reflection vector is parallel to $-x$, coincide with tetragonal cell edges labeled (ξ, η, ζ). The Bragg angle θ for a photon energy $E \approx 10.535$ eV is calculated from $\sin(\theta) \approx 0.1030\sqrt{[h^2 + k^2 + l^2/2]}$.

A structure factor for diffraction is $\Psi^K{}_Q = [\exp(i\boldsymbol{\kappa}\cdot\mathbf{d})\langle O^K{}_Q\rangle_{\mathbf{d}}]$, where the Bragg wave vector $\boldsymbol{\kappa}$ is defined by integer Miller indices (h, k, l), and the implied sum in $\Psi^K{}_Q$ is over all Re sites $\mathbf{d}$ in a unit cell of the tetragonal structure. X-ray and neutron diffraction scattering amplitudes are derived from $\Psi^K{}_Q$ with $\langle O^K{}_Q\rangle$ replaced by the appropriate type of multipole. For the paramagnetic and magnetic structures of interest, $P4_2/mnm$ and $Pnn'm'$, we obtain a generic result,

$$\Psi^K{}_Q = \left[\langle O^K{}_Q\rangle + (-1)^{h+k+l}(-1)^K\langle O^K{}_{-Q}\rangle\right]. \tag{3}$$

Recall that the time signature of multipoles $= (-1)^K$, and Re ions are subject to different site symmetries in the paramagnetic and magnetic structures. Basis allowed reflections (K even and $Q = 0$) are indexed by $h + k + l$ even. Consider ${\Psi^K}_Q$ for the basis-forbidden reflection (1, 0, 0) studied extensively by Hirai *et al.* [2]. Site symmetry for Re ions in $P4_2/mnm$ yields ${\Psi^2}_{+2} = -{\Psi^2}_{-2} = 2i\langle {t^2}_{+2}\rangle''$ while ${\Psi^2}_0 = 0$, and the first result suggests chargelike intensity is available. Looking ahead to exact scattering amplitudes in Eq. (7), no signal is predicted in the unrotated channel $(\sigma'\sigma)$ in agreement with the reported null (1, 0, 0) intensity [2]. A magnetic contribution to an amplitude may arise from Eq. (3) evaluated for $K = 1$, $Q = \pm 1$, with the result ${\Psi^1}_{+1} = {\Psi^1}_{-1} = -i\sqrt{2}\langle {t^1}_\eta\rangle$ for (1, 0, 0). Explicit results for the structure factor mentioned here evidently apply to reflections (0, 0, 3) and (0, 0, 5) that have been observed [2], and we move ahead with our results for the corresponding scattering amplitudes and azimuthal-angle scans.

To this end we exploit universal expressions for scattering amplitudes previously reported [16] and find

$$(\sigma'\sigma) = 2\sin(2\psi)\langle {t^2}_{+2}\rangle'', \quad (\pi'\pi) = \sin^2(\theta)(\sigma'\sigma), \quad (4)$$

$$(\pi'\sigma) = -(\sigma'\pi) = 2\big[-i\cos(\theta)\cos(\psi)\langle {t^1}_{+1}\rangle'' + \sin(\theta)\cos(2\psi)\langle {t^2}_{+2}\rangle''\big].$$

for (0, 0, l) with l odd. In these expressions, ψ is the angle of rotation about the reflection vector, and the ξ axis is normal to the plane of scattering at $\psi = 0$. Intensity in the rotated channel of polarization, say, is proportional to $|(\pi'\sigma)|^2$, and it includes a magnetic dipole. The latter, $\langle {t^1}_{+1}\rangle'' = -\langle {t^1}_\eta\rangle/\sqrt{2}$, is allowed different from zero in the magnetic phase, below $\approx$18 K. Diffraction in the paramagnetic phase, bracketed by temperatures $\approx$18 and $\approx$33 K [1,2], is usually referred to as Templeton-Templeton scattering, and it is solely created by the chargelike quadrupole $\langle {t^2}_{+2}\rangle''$ with $\xi\eta$-like angular symmetry.

Scattered intensity picked out by circular polarization in the primary photon beam $= P_2\Upsilon$ with [17,18]

$$\Upsilon = \{(\sigma'\pi)^*(\sigma'\sigma) + (\pi'\pi)^*(\pi'\sigma)\}'', \quad (5)$$

and the Stokes parameter P_2 (a purely real pseudoscalar) measures helicity in the primary x-ray beam. Since intensity is a scalar quantity, Υ and P_2 possess identical discrete symmetries, specifically, both scalars are time-even and parity-odd (polar). Partial intensity Υ different from zero is a signature of a chiral motif of electronic and magnetic multipoles, of course. From results in Eq. (4),

$$\Upsilon(0, 0, l) = -2\langle {t^1}_{+1}\rangle''\cos(\theta)\cos(\psi)(\sigma'\sigma)[1 + \sin^2(\theta)]. \quad (6)$$

Notably, $\Upsilon(0, 0, l)$ is an odd function of the azimuthal angle, and a nonzero value is specific to long-range magnetic order permitted by $Pnn'm'$. Figure 2 depicts $\Upsilon(0, 0, 5)$ in units of $(\langle {t^2}_{+2}\rangle''\langle {t^1}_{+1}\rangle'')$ as a function of ψ in the sector of positive values. Bragg spots (0, 0, 3) and (0, 0, 5) have been observed in resonant x-ray diffraction [2].

Next, space-group forbidden (h, k, 0) with $h + k$ odd. Let ${A^1}_1 = 2i\cos(\delta)\ \langle {t^1}_{+1}\rangle''$, ${B^1}_1 = -2\sin(\delta)\ \langle {t^1}_{+1}\rangle''$, ${A^2}_2 = -2\sin(2\delta)\ \langle {t^2}_{+2}\rangle''$, ${B^2}_2 = 2i\cos(2\delta)\ \langle {t^2}_{+2}\rangle''$, where δ is the angle subtended by the reflection vector and $-x$, e.g., $\cos(2\delta) = (h^2 - k^2)/(h^2 + k^2)$. Amplitudes are

$$(\sigma'\sigma) = -\sin^2(\psi){A^2}_2, \quad (\pi'\pi) = [1 - \sin(\theta)^2\sin^2(\psi)]{A^2}_2, \quad (7)$$

$$(\pi'\sigma) = \cos(\theta)\cos(\psi){A^1}_1 + i\sin(\theta){B^1}_1 - (1/2)\sin(\theta)\sin(2\psi){A^2}_2 + i\cos(\theta)\sin(\psi){B^2}_2.$$

Intensity of the Bragg spot (4, 1, 0) has been observed in nonresonant x-ray diffraction [2]. The corresponding intensity anticipated in resonance-enhanced diffraction in the rotated channel of polarization $|(\pi'\sigma)|^2$ is depicted in Fig. 3 for three values of the quadrupole-dipole ratio $r = (\langle {t^2}_{+2}\rangle''/\langle {t^1}_{+1}\rangle'')^2$. The evident sensitivity of $|(\pi'\sigma)|^2$ as a function of ψ to small changes in r implies that an experiment is well worth trying.

Model multipoles Eq. (2) predict $(\langle {t^2}_{+2}\rangle''/\langle {t^1}_{+1}\rangle'') = 0$ at the L_2 absorption edge, and $(\langle {t^2}_{+2}\rangle''/\langle {t^1}_{+1}\rangle'')$ is proportional to (β'/α) at the L_3 edge. As already noted, the observed magnetic moment is consistent with $(\beta'/\alpha) \sim 1$ [1]. Recall that the parameter β is restricted to purely real values ($\beta'' = 0$) in $P4_2/mnm$.

The (h, k, 0) chiral signature,

$$\Upsilon(h, k, 0) = {A^2}_2\big(\cos(\theta)\cos(\psi)\{1 - [1 + \sin^2(\theta)]\sin^2(\psi)\} \times {A^1}_1'' + \sin(\theta)[1 + \cos^2(\theta)\sin^2(\psi)]{B^1}_1\big), \quad (8)$$

is proportional to $[\langle {t^1}_\eta\rangle\langle {t^2}_{+2}\rangle'']$, and it is the same as $\Upsilon(0, 0, l)$ in this respect. However, the two signals differ as functions of the azimuthal angle, with $\Upsilon(h, k, 0)$ an even function of ψ.

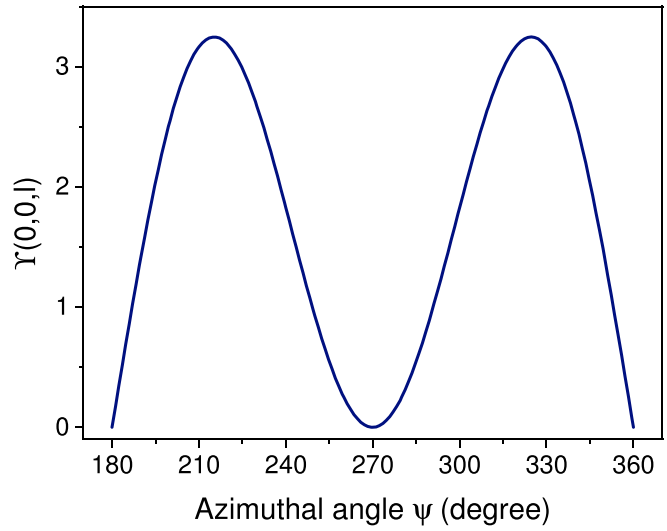

FIG. 2. The predicted chiral signature $\Upsilon(0, 0, l)$ for the Bragg spot (0, 0, 5) observed by Hirai *et al.* in resonance-enhanced x-ray diffraction [2]. Unit $(\langle {t^2}_{+2}\rangle''\langle {t^1}_{+1}\rangle'')$ used for $\Upsilon(0, 0, l)$ is taken to be positive. Azimuthal angle is in the range 180°–360° where Υ is positive. Values are derived from Eq. (6), and $\Upsilon(0, 0, 3)$ is around 3% smaller than displayed $\Upsilon(0, 0, 5)$.

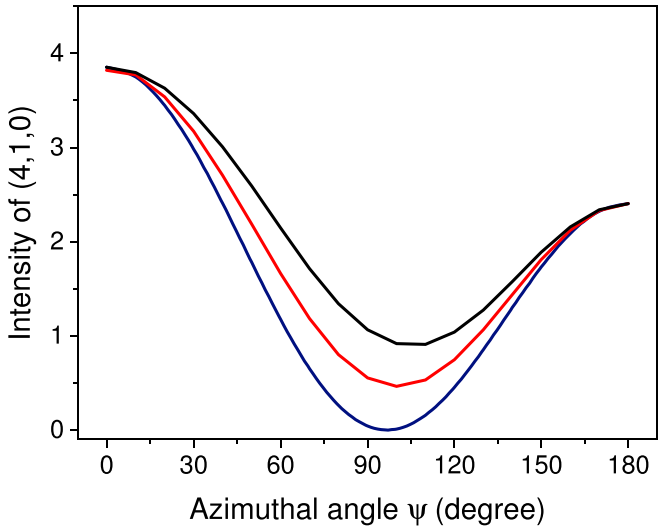

FIG. 3. Intensity $|(\pi'\sigma)|^2$ of the Bragg spot (4, 1, 0) observed by Hirai *et al.* in nonresonant x-ray diffraction, cf. Fig. 2(d) [2], calculated using Eq. (7). Azimuthal angle ψ in the range 0°–180°. Intensity scale is set by $(\langle t^1{}_{+1}\rangle'')^2$, and results are given for three values of the quadrupole-dipole ratio $r = (\langle t^2{}_{+2}\rangle''/\langle t^1{}_{+1}\rangle'')^2$, namely, $r = 0.0$ (blue), 0.2 (red), and 0.4 (black).

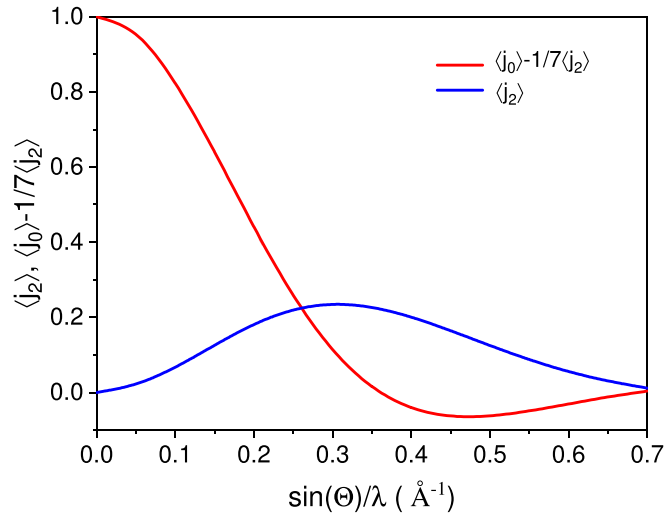

FIG. 4. Radial integrals for Re^{6+} $(5d^1)$ as a function of $\sin(\theta)/\lambda = \kappa/4\pi$ in the range 0–0.7 Å^{-1} [19]. Blue curve $\langle j_2(\kappa)\rangle$, red curve $[\langle j_0(\kappa)\rangle - (1/7)\langle j_2(\kappa)\rangle]$.

V. MAGNETIC NEUTRON DIFFRACTION

All multipoles are time-odd (magnetic), and rank $K = 1, 2, \ldots, 5$ for a d state. Even rank multipoles arise from a mixture of $j = 3/2$ and $j' = 5/2$ in Eq. (1) alone [9,11]. The present calculation retains dipoles and quadrupoles in the intermediate scattering amplitude $\langle \mathbf{Q}\rangle$ for Bragg diffraction. Multipoles for neutron scattering $\langle \boldsymbol{\tau}^K\rangle$ have a strong dependence on the magnitude of the scattering wave vector imparted through spherical Bessel functions $\langle j_n(\kappa)\rangle$ averaged over a radial wave function. The dipole $\langle \boldsymbol{\tau}^1\rangle$ is a sum of $\langle j_0(\kappa)\rangle$ and $\langle j_2(\kappa)\rangle$, and $\langle \tau^2\rangle \propto \langle j_2(\kappa)\rangle$. By definition, $\langle j_0(0)\rangle = 1$ while $\langle j_n(0)\rangle = 0$ for $n \geqslant 2$, and $\langle j_2(\kappa)\rangle$ is a maximum near $\kappa \approx 3.8$ Å^{-1} just short of the first zero in $\langle j_0(\kappa)\rangle$, cf. Fig. 4 [19].

Intensity of a Bragg spot $= |\langle \mathbf{Q}_\perp\rangle|^2$, where the operator $\mathbf{Q}_\perp = \{\kappa^{-2}[\boldsymbol{\kappa} \times (\mathbf{Q} \times \boldsymbol{\kappa})]\}$ with

$$\mathbf{Q} = \exp(i\mathbf{R}_j \bullet \boldsymbol{\kappa})[\mathbf{S}_j - \kappa^{-2}(i/\hbar)(\boldsymbol{\kappa} \times \mathbf{p}_j)], \tag{9}$$

and the implied sum is over all unpaired electrons. In Eq. (9), $\mathbf{R}$ and $\mathbf{p}$ are conjugate operators for electronic position and linear momentum, respectively. Even rank multipoles are created by the first, spin-dependent contribution, and they represent entanglement of $\mathbf{R}$ and the spin anapole $\boldsymbol{\Omega}$ [9,11]. Amplitudes for basis forbidden reflections, $h + k + l$ odd, depend on two purely real combinations of multipoles $A = -i[\langle \tau^1{}_{+1}\rangle + \langle \tau^1{}_{-1}\rangle] = -\sqrt{2}\langle \tau^1{}_\eta\rangle$, and $B = [\langle \tau^2{}_{+1}\rangle - \langle \tau^2{}_{-1}\rangle] = 2\langle \tau^2{}_{+1}\rangle'$ with $\xi\zeta$-like angular symmetry. In terms of a unit vector $(p, q, r) = \boldsymbol{\kappa}/\kappa$,

$$\langle Q_\xi\rangle \approx -pq\sqrt{3}B, \quad \langle Q_\eta\rangle \approx -(3/\sqrt{2})A + \left(p^2 - r^2\right)\sqrt{3}B,$$
$$\langle Q_\zeta\rangle \approx qr\sqrt{3}B. \tag{10}$$

The purely magnetic contribution to a Bragg diffraction pattern can be recognized by a nonzero spin-flip intensity [5,20,21],

$$\mathrm{SF} = |\langle \mathbf{Q}_\perp\rangle - \mathcal{P}(\mathcal{P} \bullet \langle \mathbf{Q}_\perp\rangle)|^2, \tag{11}$$

where $\mathcal{P} = (\mathcal{P}_\xi, \mathcal{P}_\eta, \mathcal{P}_\zeta)$ is a unit vector in the direction of the polarization in the primary neutron beam. For $\mathcal{P}$ parallel to the Bragg wave vector $\boldsymbol{\kappa}$ the result is $\mathrm{SF} = |\langle \mathbf{Q}_\perp\rangle|^2$. We shall consider the opposite extreme $\boldsymbol{\mathcal{P}} \perp \boldsymbol{\kappa}$ [21].

Intensities of Bragg spots indexed by $(0, 0, l)$ with l odd are $|\langle \mathbf{Q}_\perp\rangle|^2 = \langle \mathrm{Q}_\eta\rangle^2$, while $\mathrm{SF} = [\mathcal{P}_\xi \langle \mathrm{Q}_\eta\rangle]^2$ for $\mathcal{P}_\zeta = 0$, and $\langle \mathrm{Q}_\eta\rangle$ in Eq. (10) is a simple sum of the dipole and quadrupole. For the second class of basis forbidden Bragg spots $\boldsymbol{\kappa} = \boldsymbol{\kappa}(p, q, 0)$ we obtain

$$|\langle Q_\perp\rangle|^2 = p^2\{\sqrt{3}B - 3A/\sqrt{2}\}^2. \tag{12}$$

Intensity is zero for $\boldsymbol{\kappa}$ parallel to the crystal η axis. Since $\langle \mathrm{Q}_\zeta\rangle = 0$ for $r = 0$ one has $\mathcal{P} \bullet \langle \mathbf{Q}_\perp\rangle = 0$ and $\mathrm{SF} = |\langle \mathbf{Q}_\perp\rangle|^2$ for $\mathcal{P} = (0, 0, 1)$.

Our minimal model of the Re atomic wave function discussed in Sec. III yields the estimates

$$A = -(2\sqrt{2}/3)\langle S_\eta\rangle[\langle j_0(\kappa)\rangle - (1/7)\langle j_2(\kappa)\rangle],$$
$$B = [10/(7\sqrt{3})]\langle S_\eta\rangle\langle j_2(\kappa)\rangle. \tag{13}$$

In this model, the dipole $A \propto \langle \tau^1{}_\eta\rangle$ and quadrupole $B \propto \langle \tau^2{}_{+1}\rangle'$ are proportional to the η component of the magnetic moment. Radial integrals $[\langle j_0(\kappa)\rangle - (1/7)\langle j_2(\kappa)\rangle]$ and $\langle j_2(\kappa)\rangle$, appearing in A and B are displayed in Fig. 4 [19]. Note that, use of A in Eq. (12) returns the standard result, whereby $|\langle \mathbf{Q}_\perp\rangle|^2$ is proportional to the square of the magnetic moment in the forward direction of scattering, where $\langle j_2(\kappa)\rangle \approx 0$.

VI. DISCUSSION AND CONCLUSIONS

In summary, we have studied consequences of a cubic-to-tetragonal structural transition and magnetic long-range

order reported at temperatures ≈33 and ≈18 K, respectively, in Ba_2MgReO_6 [1,2]. Our analysis of the structural transition and site symmetries reveals order of a lone E_g-type quadrupole, while E_g and T_{2g} types are permitted with onset of long-range magnetic order. Rhenium site symmetry remains centrosymmetric, and Dirac multipoles are thereby forbidden. The magnetic motif, illustrated in Fig. 1, is composed of ferro- and antiferromagnetic orders of conventional magnetic dipoles. Notably, the corresponding space-group $Pnn'm'$ (No. 58.398) allows the structural distortions with the tetragonal $P4_2/mnm$ symmetry, i.e., there must be a coupling between the two magnetic orders and structural distortion. The foregoing essential properties and classifications of structural and magnetic orders in Ba_2MgReO_6 are absent in a published report of high-resolution x-ray Bragg diffraction patterns [2].

Furthermore, our magnetic space-group allows a chiral signature caused by interference between a magnetic dipole and an electronic quadrupole in resonant x-ray Bragg diffraction (intensity enhanced by an electric dipole–electric dipole (E1-E1) absorption event). Amplitudes in all four channels of polarization contribute to the chiral signature, and corresponding individual intensities are shown to carry useful information that merit experimental investigation. X-ray data to hand were gathered at the L_3 absorption edge [2]. Experimental studies of other compounds hosting heavy transition ions have encountered very different intensities between L_2 and L_3 absorption edges.

Contributions to Bragg spots in magnetic neutron diffraction that violate the F-centring condition include a quadrupole exclusive to mixing of $5d^1$ Re manifolds. Based on current knowledge of heavy transition metal ions in an almost octahedral environment, this result is expected. Physically, the quadrupole hallmarks entanglement of anapole and spatial degrees of freedom. Magnetic intensity picked out in neutron polarization analysis is here calculated for all allowed dipoles and quadrupoles. Quadrupoles in x-ray and neutron diffraction amplitudes are predicted to have different angular symmetries, since the former is purely electronic and the latter purely magnetic.

A plausible rhenium atomic wave function introduced in Sec. III is used to estimate saturation values of all multipoles in our amplitudes for x-ray and neutron scattering. The previously measured magnetic moment is a guide to values of the two unknowns in the wave function [2]. Site symmetry demands a null value for one of the unknowns in the paramagnetic phase defined by $P4_2/mnm$.

ACKNOWLEDGMENT

Dr. Y. Tanaka advised us on the feasibility of resonant x-ray Bragg diffraction.

[1] D. Hirai and Z. Hiroi, J. Phys. Soc. Jpn. **88**, 064712 (2019).
[2] D. Hirai, H. Sagayama, S. Gao, H. Ohsumi, G. Chen, Taka-h. Arima, and Z. Hiroi, Phys. Rev. Res. **2**, 022063(R) (2020).
[3] D. D. Maharaj, G. Sala, M. B. Stone, E. Kermarrec, C. Ritter, F. Fauth, C. A. Marjerrison, J. E. Greedan, A. Paramekanti, and B. D. Gaulin, Phys. Rev. Lett. **124**, 087206 (2020).
[4] S. W. Lovesey and D. D. Khalyavin, Phys. Rev. B **102**, 064407 (2020).
[5] G. J. Nilsen, C. M. Thompson, C. Marjerisson, D. I. Badrtdinov, A. A. Tsirlin, and J. E. Greedan, Phys. Rev. B **103**, 104430 (2021).
[6] S. W. Lovesey, D. D. Khalyavin, G. van der Laan, and G. J. Nilsen, Phys. Rev. B **103**, 104429 (2021).
[7] S. Gao, D. Hirai, H. Sagayama, H. Ohsumi, Z. Hiroi, and T.-H. Arima, Phys. Rev. B **101**, 220412(R) (2020).
[8] S. W. Lovesey, E. Balcar, K. S. Knight, and J. Fernández Rodríguez, Phys. Rep. **411**, 233 (2005).
[9] S. W. Lovesey, Phys. Scripta **90**, 108011 (2015).
[10] S. W. Lovesey *et al.*, Phys. Rev. Lett. **122**, 047203 (2019).
[11] D. D. Khalyavin and S. W. Lovesey, Phys. Rev. B **100**, 224415 (2019).
[12] Y. Joly, Y. Tanaka, D. Cabaret, and S. P. Collins, Phys. Rev. B **89**, 224108 (2014).
[13] We use the BNS setting of magnetic space groups, see Bilbao Crystallographic server, http://www.cryst.ehu.es.
[14] B. T. Thole, P. Carra, F. Sette, and G. van der Laan, Phys. Rev. Lett. **68**, 1943 (1992); P. Carra, B. T. Thole, M. Altarelli, and X. D. Wang, *ibid.* **70**, 694 (1993); P. Carra, H. König, B. T. Thole, and M. Altarelli, Physica B **192**, 182 (1993).
[15] L. C. Chapon and S. W. Lovesey, J. Phys.: Condens. Matter **23**, 252201 (2011).
[16] V. Scagnoli and S. W. Lovesey, Phys. Rev. B **79**, 035111 (2009).
[17] S. W. Lovesey and V. Scagnoli, J. Phys.: Condens. Matter **21**, 474214 (2009).
[18] A. Rodríguez-Fernández, J. A. Blanco, S. W. Lovesey, V. Scagnoli, U. Staub, H. C. Walker, D. K. Shukla, and J. Strempfer, Phys. Rev. B **88**, 094437 (2013).
[19] K. Kobayashi, T. Nagao, and M. Ito, Acta. Crystallogr. Sect. A **67**, 473 (2011).
[20] R. M. Moon, T. Riste, and W. C. Koehler, Phys. Rev. **181**, 920 (1969).
[21] J. Jeong, B. Lenz, A. Gukasov, X. Fabreges, A. Sazonov, V. Hutanu, A. Louat, D. Bounoua, C. Martins, S. Biermann, V. Brouet, Y. Sidis, and P. Bourges, Phys. Rev. Lett. **125**, 097202 (2020).